ACS APPLIED MATERIALS & INTERFACES

Research Article

www.acsami.org

Tunable Solubility Parameter of Poly(3-hexyl thiophene) with Hydrophobic Side-Chains to Achieve Rubbery Conjugated Films

Seulyi Lee,[†,§] Hyeonyeol Jeon,[‡,§] Mi Jang,[†] Kyung-Youl Baek,[‡] and Hoichang Yang*[,†]

[†]Department of Applied Organic Materials Engineering, Inha University, Incheon 402-751, Korea

[‡]Center for Materials Architecturing, Korea Institute of Science and Technology, Seoul 136-794, Korea

Supporting Information

ABSTRACT: A highly π-conjugated nanofibrillar network of poly(3-hexyl thiophene) (P3HT) embedded in polydimethylsiloxane (PDMS) elastomer films on SiO_2 dielectrics was facilely developed via solution-blending of an ultrasound-assisted dilute P3HT solution with a PDMS precursor followed by spin-casting and curing. In contrast, simple blending without ultrasonication against the dilute P3HT solution yielded large agglomerates in cast films owing to a great difference in solubility parameter (δ) values (P3HT = 9.5 $cal^{1/2}$ $cm^{-3/2}$, PDMS = 7.3 $cal^{1/2}$ $cm^{-3/2}$). In the ultrasound-assisted 0.1 vol % P3HT solutions, the π-conjugated polymer could develop crystalline nanofibrils surrounded by nonpolar hexyl side chains with the same δ value as that of PDMS, yielding homogeneously dispersed 10 wt % loaded P3HT/PDMS blend films. Spun-cast P3HT/PDMS blend films could yield high electrical properties in organic field-effect transistor, including mobilities of up to 0.045 cm^2 V^{-1} s^{-1} and on/off current ratios of $>5 \times 10^5$, as well as excellent environmental stability owing to the outer PDMS layer.

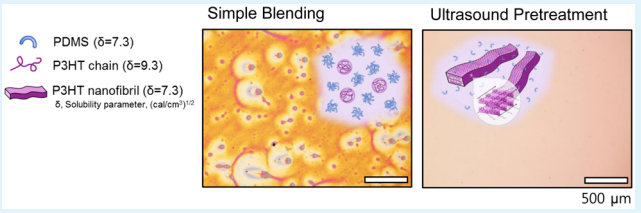

KEYWORDS:
ultrasonication, solubility parameter, miscibility, directed self-assembly, poly(3-hexyl thiophene), organic field-effect transistor

1. INTRODUCTION

Organic field-effect transistors (OFETs) based on conjugated polymers have attracted extensive interest because various solution processing methods, such as casting, inkjet, gravure, and roll-to-roll printing, can be applied for their fabrication.[1,2] Many π-conjugated polymers, including poly(3-alkyl thiophene)s, (P3AT)s,[3,4] poly(2,5-bis(3-alkylthiophen-2-yl)-thieno[3,2-*b*]thiophene) (pBTTT),[5,6] and poly(3,3‴-didodecylquaterthiophene) (PQT-12),[7,8] as well as conjugated copolymers with donor−acceptor ($D-A$) architectures, such as diketopyrrolopyrrole (DPP)-based copolymers,[9,10] have been synthesized and used for high-performance OFETs. Most polymer FETs can be applied in low-cost high-throughput microelectronics such as smart cards, simple displays, sensors, and electronic barcodes.[11−15] It is known that, due to polymeric long-chain backbone and conjugated rigidity, solution-processed semiconducting polymers require sufficient casting time to achieve highly π-conjugated structures along the source/drain (S/D) electrodes in the polymer FETs. Additionally, the well-controlled interface between the organic semiconductor and gate insulator is essential to achieve high device performance because the charge transport occurs within several nanometers thick layer near the dielectric.[16,17]

Blends and other multicomponent systems have been used in various polymer applications to satisfy multiple requirements that cannot be fulfilled by a single material. Recently, multicomponent semiconducting channel systems incorporating mechanically tough polymers have been developed to enhance the capability for formability and flexibility of OFETs. Specifically, poly(3-butyl thiophene),[18,19] poly(3-hexyl thiophene) (P3HT),[20−22] and PQT-12[23,24] were blended with insulating or encapsulating matrix polymers. Such bicomponent blending can drastically reduce the minimum amounts of semiconducting polymers required to form uniform coating layer onto substrates, providing low-cost processing benefits and single processing advantages for encapsulation/or insulation/channel coating via selectively vertical phase-segregation of the π-conjugated polymers.[18−26] Since the semiconducting blends possess much higher complexity than single semiconducting polymer systems, it is necessary to systematically investigate the phase separation, which affects the physical and electrical properties of the semiconductor/insulator blended films in OFETs. In particular, semiconducting-elastomer blend films can offer expanded flexibility for OFETs, as well as reduced materials cost and improved mechanical properties. However, it is still difficult to fabricate homogeneous semiconducting/elastomer blend films owing to the large differences in the solubility parameter (δ) between these components.[27]

Here, we investigated bicomponent blends composed of well-controlled P3HT nanofibrils and polydimethylsiloxane (PDMS) elastomer matrix, using the following steps: (1) ultrasound-assisted crystal segregation of P3HT from its dilute solution, (2) blending with a PDMS precursor, and (3) spin-

Received: October 28, 2014
Accepted: December 22, 2014
Published: December 22, 2014

DOI: 10.1021/am507512m
ACS Appl. Mater. Interfaces 2015, 7, 1290−1297

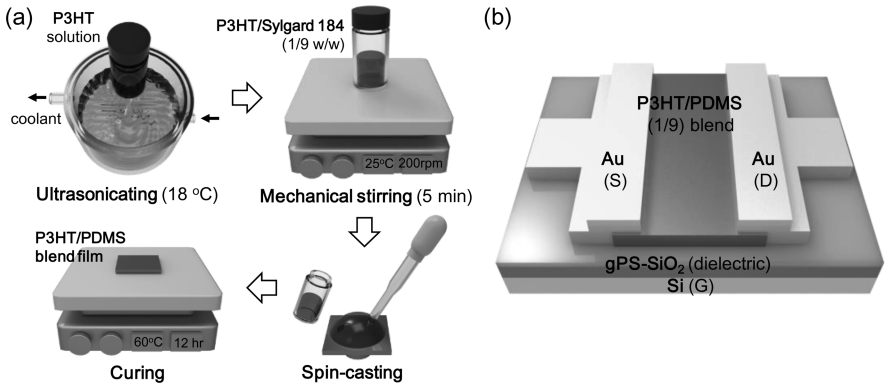

Figure 1. Scheme of (a) ultrasonication-based film fabrication of P3HT/PDMS blend and (b) a top-contacted electrode OFET containing a P3HT film spun-cast onto the gPS-SiO_2 gate dielectric.

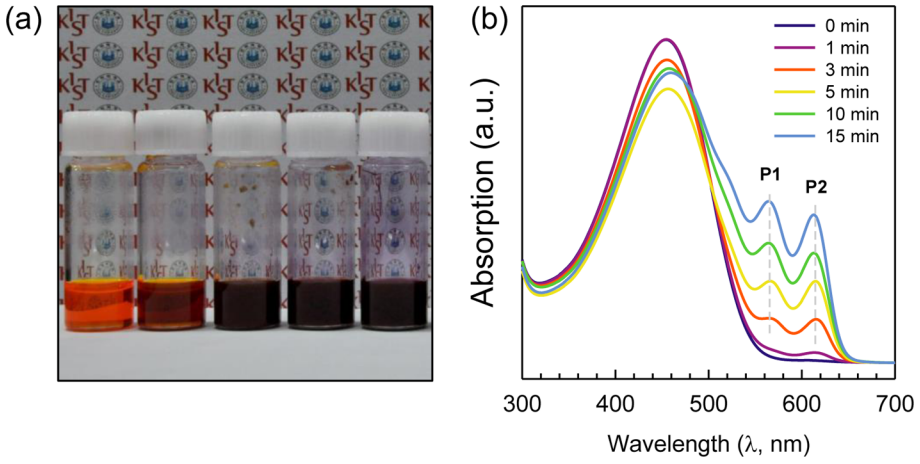

Figure 2. (a) Optical color and (b) UV−vis spectrum changes of the ultrasound-assisted 0.1 vol % P3HT solution as a function of t_{sonic}.

casting onto a polymer-treated SiO_2 dielectric. A simple solution blending of P3HT and PDMS with discernible δ values of 9.5 and 7.3 $cal^{1/2}$ $cm^{-3/2}$, respectively, yielded macro phase-separated domains in both the solution and solid states. In contrast, optimization of ultrasonication-based solution processing produced optically uniform and smooth P3HT/PDMS blend films (1/9 in w/w). In these films, P3HT nanofibrils could be embedded, well-dispersed, and percolated in the elastomer matrix, yielding high electrical properties in OFET, specifically, a field-effect mobility (μ_{FET}) value of ~0.045 cm^2 V^{-1} s^{-1} and on/off current ratio (I_{ON}/I_{OFF}) of >5 × 10^5. Additionally, these films led to negligible hysteresis and environmental stability by encapsulating the channel of the PDMS matrix. Ultrasound treatment to induce directed self-assembly of π-conjugated polymers in a dilute solution revealed that the reduced differences of δ values between semiconducting and amorphous polymers can induce uniformly dispersed charge-transport paths in a nonpolar polymer matrix, such as PDMS, expanding flexibility and enabling realization of high-performance OFET architectures at drastically reduced materials cost with improved mechanical properties.

2. EXPERIMENTAL SECTION

2.1. Materials and Sample Preparation. P3HT was synthesized by the Grignard metathesis method with Ni(dppp)Cl_2 catalyst,[28] and its number-average molecular weight (M_n), weight-average molecular weight (M_w), molecular weight distribution (PDI, M_w/M_n), and regioregularity (RR) were determined by a Gel permeation chromatograph (GPC, calibrated with polystyrene (PS) standards, JASCO SEC System with RI-2031 and UV-2075 in tetrahydrofuran at 40 °C with a rate of 1 mL min^{-1}) and ^1H nuclear magnetic resonance (NMR, Bruker Ascend 400 MHz in $CDCl_3$ at 25 °C) analyses (see Figure S1 in Supporting Information, SI). A PDMS elastomer kit (Sylgard 184, Dow Chemical) was used without any purification. 300 nm thick SiO_2 layers on heavily n-doped Si substrates were first cleaned with acetone, isopropanol, and UV−ozone (UV−O_3) exposure. Next, dimethylchlorosilane (-Si(CH_3)$_2$Cl)-terminated PS (M_n = 8.5 kDa, PDI = 1.07, Polymer Sources, Inc.) as a surface modifier was chemically grafted to the UV−O_3-treated SiO_2 surfaces as previously described.[29] The grafted PS-SiO_2 dielectrics (referred to as gPS-SiO_2) were used as bilayer gate dielectrics.

P3HT (M_n = 21 kDa and PDI = 1.19) was completely dissolved in toluene at 60 °C to prepare 1 mg·ml^{-1} solution. Different nanoscale agglomerates of P3HT were generated in solutions kept at 18 °C via ultrasonication for 0−15 min (NXPC-4020, 40 kHz, 400 W). The ultrasound-assisted solutions and PDMS precursor kit were then simply blended to give P3HT/PDMS ratios of 1/9 in weight, after which they were mechanically stirred at room temperature for 5 min. Next, 50−80 nm thick semiconducting blend films were spun-cast onto gPS-SiO_2/Si substrates from solutions and thermally treated at 60 °C for 4 h to cure the PDMS prepolymer (see Figure 1a). All procedures were performed under a glovebox (O_2 < 0.1 ppm and H_2O < 0.1 ppm). Finally, top-contacted *S*/*D* Au electrodes were thermally evaporated on either the P3HT or P3HT/PDMS blend films through a shadow mask: with a channel length (L) and width (W) of 100 and 1500 μm, respectively (see Figure 1b).

2.2. Characterization. The electrical parameters of P3HT OFETs were measured using a Keithley 4200 SCS parameter analyzer under a N_2-purged glovebox (O_2 < 0.1 ppm and H_2O < 0.1 ppm). The μ_{FET}

DOI: 10.1021/am507512m
ACS Appl. Mater. Interfaces 2015, 7, 1290−1297

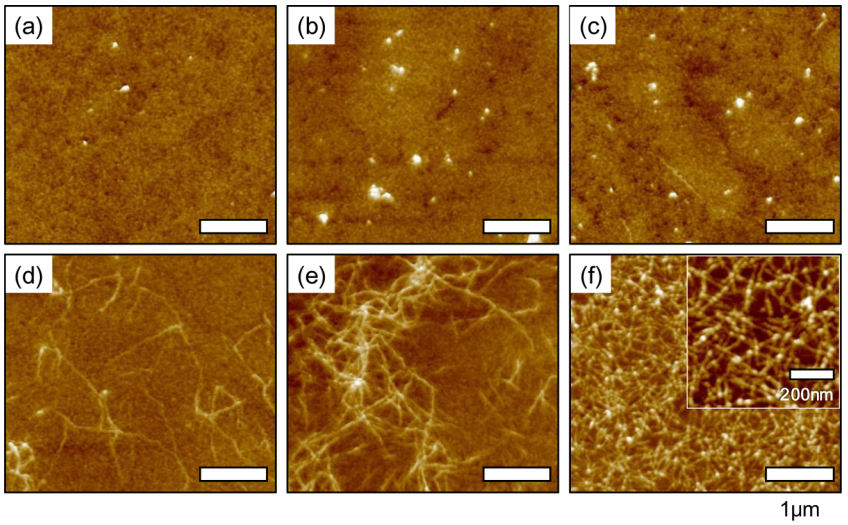

Figure 3. AFM topographies of P3HT agglomerates collected on SiO_2 substrates via spin-casting of different t_{sonic}-treated P3HT solutions: t_{sonic} = (a) 0 min; (b) 1 min; (c) 3 min; (d) 5 min; (e) 10 min; (f) 15 min.

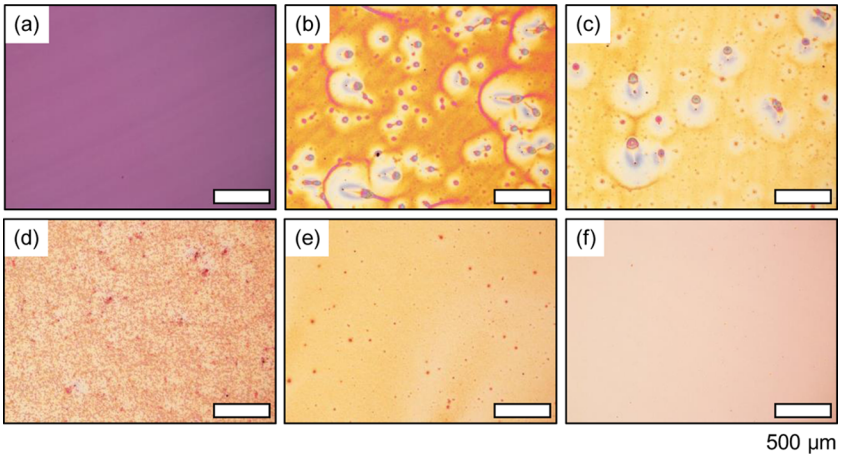

Figure 4. OM images of (a) P3HT and (b–f) 10 wt % P3HT-loaded PDMS blend films spun-cast on gPS-SiO_2 substrates from blended solutions containing different t_{sonic}-treated P3HT solutions: (a, b) 0 min; (c) 3 min; (d) 5 min; (e) 10 min; (f) 15 min.

and threshold voltage (V_{th}) were calculated in the saturation regime (drain voltage, V_D = −40 V) using the following equation: $I_D = (W/2L)\mu_{FET}C_i(V_G - V_{th})^2$, where I_D, V_G, and C_i are the drain current, gate voltage, and capacitance of the dielectrics, respectively. The C_i of the polymer-treated-SiO_2 dielectrics was approximately 10.8 nFcm^{-2}. Atomic force microscopy (AFM, Multimode Nanoscope 8, Bruker) was performed for the P3HT/PDMS cast films on the dielectric substrates using a tapping-mode probe tip (spring constant: 20–30 N m^{-1}, resonance frequency: 275–315 kHz). A UV–vis experiment (JASCO, V-670 spectrophotometer) was performed for P3HT solutions before and after ultrasonication. Two-dimensional (2D) grazing-incidence X-ray diffraction (GIXD) for the P3HT/PDMS blend films was also performed at beamline 9A of the Pohang Acceleration Laboratory (PAL, Korea). The sample was mounted on a three-axis goniometer, and the scattered intensity was recorded using a 2D detector.

3. RESULTS AND DISCUSSION

It is well-known that an ultrasonication is useful for dispersal of polymeric solutes in organic solvents. Semiconducting polymers with strong π–π interactions were recently reported to be capable of self-assembly into the intermolecular-stacked nanocrystallites in solutions when high-energy ultrasound waves were applied to untie the entangled conjugated chains.[30,31] Several groups have reported that ultrasound-assisted P3HT solutions yielded an interconnected network of P3HT nanofibrils when P3HT films were cast on gate dielectrics, even under rapid solvent-evaporation conditions.[30−32]

Here, 0.1 vol % P3HT solutions dissolved in toluene were tightly sealed in vials and subjected to ultrasound treatment inside a coolant-circulated double jacketed beaker kept at 18 °C for different times (t_{sonic}) ranging from 0 to 15 min. The visual colors of the ultrasound-assisted P3HT solutions rapidly changed from bright orange to dark red at above t_{sonic} = 1 min (see Figure 2a). Owing to the strong UV–vis absorption of dissolved P3HT at 460 nm, the ultrasound-assisted P3HT solutions showed two additional peaks around P1 = 564 nm and P2 = 613 nm (see Figure 2b), corresponding to 0–1 and 0–0 absorption energies during the π–π^* electronic transition, respectively.[33] The UV–vis peak intensities increased monotonically with an increase in t_{sonic}, and this trend exactly matched the t_{sonic}-dependent crystal growth and development of P3HT from nanorods to nanofibrils.

Figure 3 represents AFM topographies of the P3HT crystallites collected from ultrasound-assisted solutions. The

DOI: 10.1021/am507512m
ACS Appl. Mater. Interfaces 2015, 7, 1290–1297

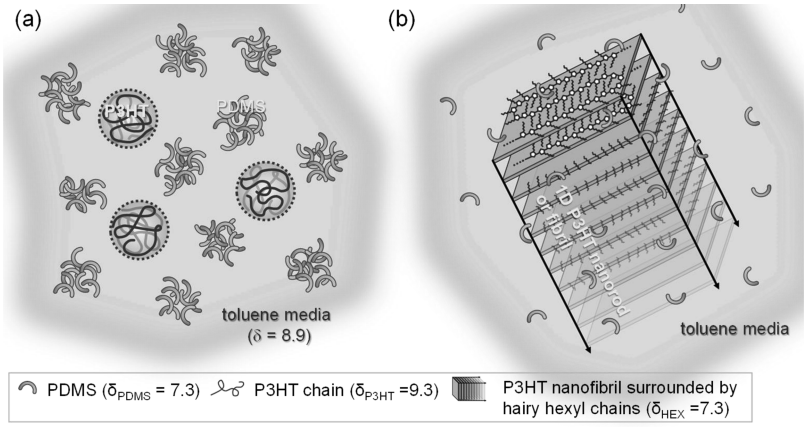

Figure 5. Schematic diagrams: (a) macro phase-separation behavior of P3HT and PDMS based on the discernible δ values between these components and (b) dispersed 1D P3HT crystallites containing hairy hexyl covered surfaces in the toluene media.

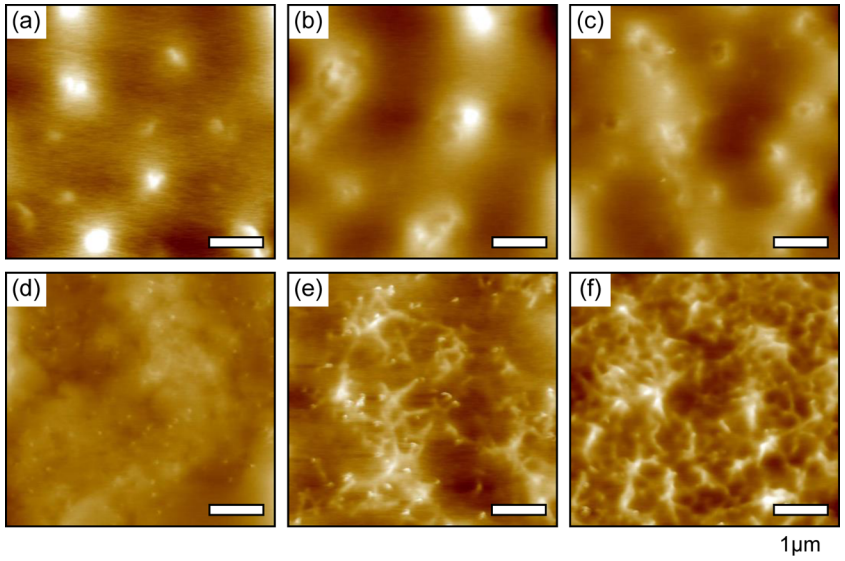

Figure 6. AFM topographies of 10 wt % P3HT-loaded PDMS blend films spun-cast on the *g*PS-SiO_2 substrates from mixtures blended with the P3HT solutions treated for different t_{sonic}: (a) 0 min; (b) 1 min; (c) 3 min; (d) 5 min; (e) 10 min; (f) 15 min.

ultrasound wave applied to the P3HT solutions could quickly develop one-dimensional (1D) crystal structures with *face-to-face* multistacking between conjugated thiophene backbone chains, as well as hairy hexyl side-chains vertically oriented along the crystal growth direction. In the ultrasound-assisted solutions, the 1D nanorods or nanofibrils of P3HT were suspended, and the portion of dissolved P3HT chains decreased drastically with an increase in t_{sonic}.[34,35] These results strongly support that the conjugation length and ordering of P3HT chains in the dilute solutions via ultrasonication were significantly enhanced as previously reported.[31]

To prepare P3HT/PDMS bicomponent solutions, the PDMS precursor was added to different t_{sonic}-treated P3HT solutions, and the blended solutions were then mechanically stirred for 5 min. The blended solutions were subsequently spun-cast onto the gPS-SiO_2 dielectrics, after which the resulting films were thermally treated at 60 °C for 4 h to cure the PDMS matrix. Figure 4 shows optical microscopy (OM) images of 50−80 nm thick P3HT only and P3HT/PDMS (1/9 w/w) blend films cast on the gPS-SiO_2 dielectrics. P3HT-only film spun-cast from toluene was clear and featureless in the OM image (see Figure 4a). In contrast, OM images of the ultrasound-assisted P3HT/PDMS blend films showed morphologies that ranged from macroseparated agglomerates to those with no feature depending on t_{sonic}. When there was no ultrasound irradiation, simply blended solutions (t_{sonic} = 0 min) yielded agglomerates of several tens of micrometers in the spun-cast film (see Figure 4b). In particular, the pinning effect around these agglomerates on the gPS-SiO_2 dielectric seriously degraded the uniformity of the cast films. However, the ultrasound-assisted P3HT ($t_{sonic} \geq$ 3 min) and PDMS blend solutions produced uniformly dispersed phases of P3HT in the as-spun films (see Figure 4c−f). Interestingly, the blend film fabricated from the 15 min-ultrasonicated P3HT solution was optically clear (Figure 4f).

As shown in Figure 4, the miscibility between the P3HT (δ_{P3HT} = 9.50 $cal^{1/2}$ $cm^{-3/2}$) and PDMS (δ_{PDMS} = 7.30 $cal^{1/2}$ $cm^{-3/2}$) was drastically improved via the ultrasonication of P3HT solutions. The results were primarily related to the molecular architecture of P3HT containing both polar and nonpolar segments. The δ values of the thiophene backbone and hexyl side chain were reported as δ_{Th} = 9.80 $cal^{1/2}$ $cm^{-3/2}$ and $\delta_{HEX} \approx$ 7.30 $cal^{1/2}$ $cm^{-3/2}$, respectively.[34,36,37] Note that most materials with similar δ values are likely to be miscible in

DOI: 10.1021/am507512m
ACS Appl. Mater. Interfaces 2015, 7, 1290−1297

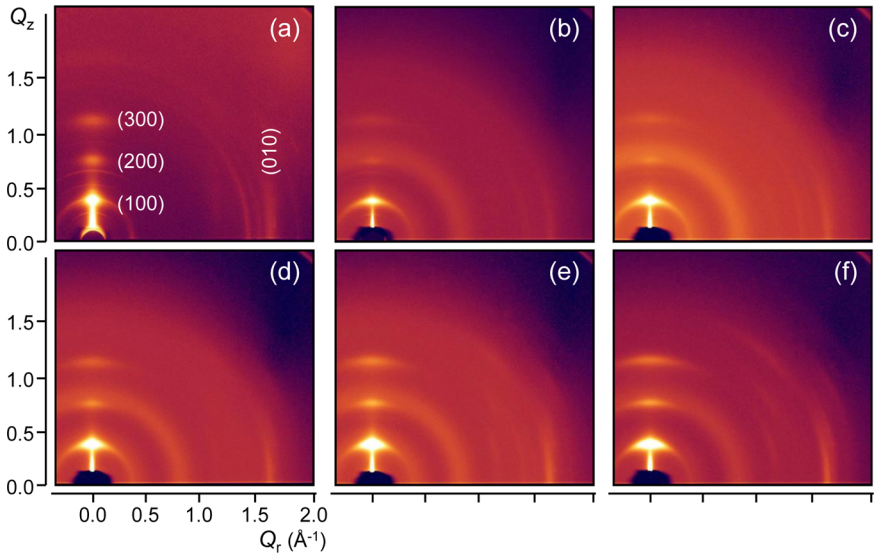

Figure 7. 2D GIXD patterns of (a) 100% P3HT and (b–f) 10 wt % P3HT-loaded PDMS blend films spun-cast on gPS-SiO_2 substrates from mixtures based on the P3HT solutions pretreated with different t_{sonic}: (a, b) 0 min; (c) 1 min; (d) 5 min; (e) 10 min; (f) 15 min.

both the dissolved and solid states. Owing to the large value of $\Delta\delta$ (= $\delta_{P3HT} - \delta_{PDMS}$) of 1.80 $cal^{1/2}$ $cm^{-3/2}$, it is possible that the P3HT and PDMS components became easily immiscible in toluene, after which large portions of PDMS formed micelles containing fewer P3HT chains (see Figure 5a). Unlike the coil-like conformation of P3HT chains, nanocrystallites burying π-conjugated thiophene backbones may be easily surrounded by PDMS precursor owing to $\delta_{HEX} \approx \delta_{PDMS}$. In the toluene media ($\delta_{TOL}$ = 8.9 $cal^{1/2}$ $cm^{-3/2}$), the crystal surfaces covered by hairy hexyl chains can have much greater attraction to PDMS than toluene molecules (Figure 5b).

To characterize the ultrasound pretreatment effects of the P3HT solutions on the dispersion and percolation of semiconducting nanocrystallites in the resulting blend films, AFM was also performed on the spun-cast P3HT/PDMS films (50–80 nm thickness). Because of the rubbery surface character of the blend films, a harder AFM tapping force was applied with a driving amplitude of greater than three times the initial one of a standard AFM probe (see Supporting Information, Figure S2). The P3HT domains buried inside the PDMS matrix improved the environmental stability of P3HT (discussed below), despite lack of vertical-phase-separation mechanisms known to impart similar benefits.[25,38,39]

Figure 6 shows typical AFM topographies of ultrasound-assisted P3HT/PDMS (1/9) blend films on the gPS-SiO_2 gate dielectrics. As expected from the OM morphologies (see Figure 4), the nanoscale miscibility between P3HT and PDMS was considerably enhanced via the ultrasound-assisted self-assembly of P3HT in the solutions. In the P3HT/PDMS blend films, the degree of the inhomogeneity and agglomerated phases decreased significantly as t_{sonic} increased for the dilute P3HT solution. As a result, homogeneous films could be reproducibly spun-cast from the 15 min ultrasound-assisted P3HT solution blended with the PDMS: the highly percolated network of the P3HT crystal nanofibrils could extend the π-conjugation path for charge-carrier transport (see Figure 6f).

Additionally, synchrotron-based GIXD was performed on all the spun-cast films to clarify the π-conjugated structures of P3HT crystallites embedded in the blend films. Figure 7 shows the 2D GIXD patterns of as-spun 100% P3HT and 10% P3HT-loaded PDMS blend films on the gPS-SiO_2 dielectrics. As reported elsewhere,[40,41] the 2D GIXD pattern of the spun-cast P3HT film showed broad X-ray reflection peaks of (l00) and (010) crystal planes along the Q_z and Q_r axes, respectively (see Figure 7a), indicating that π-conjugated planes were laterally less-ordered on the substrate owing to rapid solvent evaporation. In the blend films, both the crystallinity and π-conjugated chain orientation on the dielectrics increased drastically with an increase in t_{sonic} against the P3HT solutions (see Supporting Information, Figure S3), while the no-ultrasonic system showed weak crystal reflections and a broad amorphous hollow in the 2D GIXD pattern originating from P3HT and PDMS, respectively (see Figure 7b–f). On the basis of the AFM and 2D GIXD results, facile ultrasound irradiation against a dilute P3HT solution and subsequent mixing of the solutions with PDMS precursor could develop highly crystalline structures of P3HT in these spun-cast films.

Top-contacted electrode OFETs were fabricated via thermal evaporation of Au through a shadow mask (L = 100 μm; W = 1500 μm) onto P3HT and P3HT/PDMS films (see Figure 8a). Figure 8a,b show the drain current–gate voltage (I_D–V_G) transfer curves of these OFETs based on the gPS-SiO_2 dielectric series operated under a saturation regime (drain voltage, V_D = −40 V). The electrical characteristics of the OFETs are also summarized in Table 1. First, 21 kDa P3HT OFETs showed μ_{FET} = 0.03 cm^2 V^{-1} s^{-1} and V_{th} = −4 V, with a negligible hysteresis during the V_G sweep (see Figure 8a). In contrast, the P3HT/PDMS blend films showed different electrical properties in OFETs as a function of t_{sonic}. As expected, the P3HT/PDMS blend films containing isolated P3HT agglomerates, such as the 3 min ultrasound-treated sample showed poor μ_{FET} values of below 10^{-3} cm^2 V^{-1} s^{-1} and large V_G-sweep hysteresis (see Figure 8b). However, as the P3HT nanofibrils became well-dispersed and started to be interconnected in the PDMS matrix, the electrical performance of the resulting P3HT/PDMS OFETs was significantly improved, with a μ_{FET} value of up to 0.045 cm^2 V^{-1} s^{-1} and on and off current ratio I_{ON}/I_{OFF} of >5 × 10^5, encompassing those of spun-cast P3HT OFET. The corresponding I_D–V_D output curves of the ultrasound-assisted P3HT/PDMS-based

DOI: 10.1021/am507512m
ACS Appl. Mater. Interfaces 2015, 7, 1290–1297

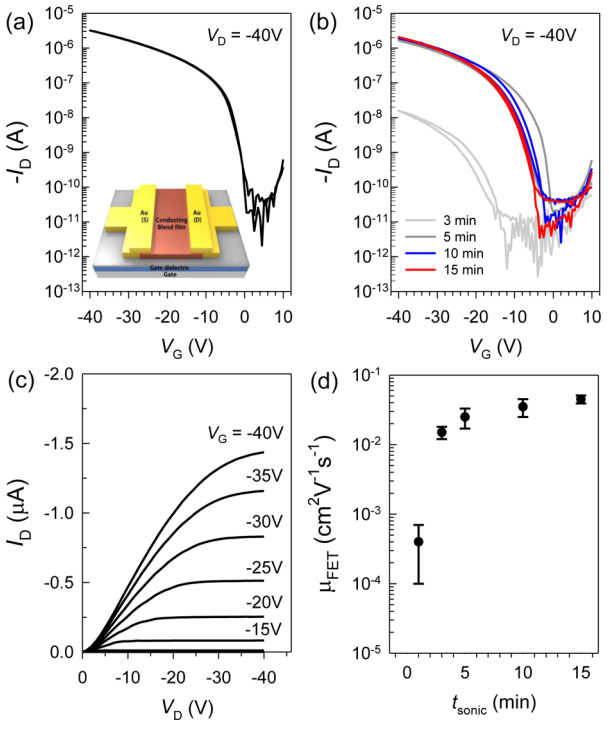

Figure 8. (a,b) Drain current-gate voltage (I_D–V_G) transfer curves of (a) spun-cast P3HT and (b) P3HT/PDMS (1/9 w/w) OFETs on gPS-SiO_2 dielectrics from the ultrasound-assisted solutions with different t_{sonic}. (c) I_D–V_D output curves of the 15 min ultrasound-assisted P3HT/PDMS based OFET. (d) Variations in μ_{FET} of P3HT/PDMS OFETs as a function of t_{sonic}.

Table 1. Electrical Performance of the P3HT and Ultrasound-Assisted P3HT/PDMS OFETs

active layer	ultrasonication time (t_{sonic}, min)	μ_{FET} (cm^2 V^{-1} s^{-1})	V_{th} (V)	I_{ON}/I_{OFF}
100% P3HT	0	0.03 ± 0.005	−4	~ 10^5
P3HT/PDMS (1/9) blend	3	<0.001	−14	>10^3
	5	0.015 ± 0.003	−4	<10^5
	10	0.025 ± 0.008	−8	~ 10^5
	15	0.045 ± 0.010	−9	>5 × 10^5

OFET showed a typical S-shape at a low V_D regime. The initial contact resistance was mainly related to the topmost thin PDMS layer, as the insulating layer between the P3HT crystallites and electrodes. Development of the conductive P3HT network inside the PDMS insulating matrix could improve the charge-carrier transport in the OFETs, especially for those blends with low P3HT content (10 wt %). Additionally, the t_{sonic} = 15 min sample showed excellent environmental stability, during continuous V_G-sweep operation in ambient air owing to the PDMS-surrounding channel, in comparison to 100% P3HT OFET showing the large negative V_{th} shift (see Supporting Information, Figure S4). We believe that these types of semiconducting-elastomer blends offer expanded flexibility for realizing high-performance OFET architectures at drastically reduced materials cost with improved deformability and flexibility.

4. CONCLUSION

Using immiscible polymeric semiconductor and insulating materials, we successfully demonstrated that bicomponent semiconducting blend films comprising well-controlled poly(3-hexyl thiophene) (P3HT) nanofibrils and polydimethylsiloxane (PDMS) elastomer matrix could be fabricated via the following steps: (1) ultrasound-assisted crystal segregation of P3HT from its dilute solution, (2) sequential blending with a PDMS precursor, and (3) spin-casting on a PS-grafted SiO_2 bilayer dielectric. A simple solution blending of P3HT and PDMS with discernible δ values of 9.50 and 7.30 $cal^{1/2}$ $cm^{-3/2}$, respectively, yielded macro phase-separated agglomerates of P3HT in both solution and solid state. Inducing one-dimensional (1D) P3HT nanocrystallites surrounded by nonpolar hexyl side chains in an ultrasound-assisted solution resulted in drastically improved miscibility of P3HT crystallites with PDMS precursor in solutions that could produce optically uniform and smooth P3HT/PDMS blend films. In this case, the 10 wt %-loaded P3HT nanofibrils could be embedded, well-dispersed, and percolated in the elastomer matrix, showing high electrical properties in OFET, with a field-effect mobility (μ_{FET}) value of ~0.045 cm^2 V^{-1} s^{-1} and on/off current ratio (I_{ON}/I_{OFF}) of >5 × 10^5, as well as negligible hysteresis and environmental stability by encapsulating the channel of the PDMS matrix.

We believe that the reduced differences in δ values between semiconducting and amorphous polymers generated by direction of self-assembly of π-conjugated polymers in dilute solution can induce uniformly dispersed charge-transport paths in a rubbery insulating polymer matrix, expanding an excellent flexibility for the realization of high-performance OFET architectures at drastically reduced materials cost with improved mechanical properties.

■ ASSOCIATED CONTENT

Supporting Information

GPC curve and ^{1}H NMR spectrum of regioregular P3HT; AFM topographies of an ultrasound-treated P3HT/PDMS spun-cast film obtained with different tapping forces; I_D–V_G transfer curves of 100% P3HT and 10 wt % P3HT-loaded PDMS OFETs operated in an ambient condition. This material is available free of charge via the Internet at http://pubs.acs.org.

■ AUTHOR INFORMATION

Corresponding Author

*E-mail: hcyang@inha.ac.kr. Phone: +82-32-860-7494.

Author Contributions

§S.L. and H.J contributed equally.

Notes

The authors declare no competing financial interest.

■ ACKNOWLEDGMENTS

This work was supported by grants from the Center for Advanced Soft Electronics under the Global Frontier Research Program (2012M3A6A5055225) and General Research Program (2013R1A12063963) of the Ministry of Education, Science, and Technology (MEST), Korea. Also, it was supported by the INHA Research Grant (INHA-50278-01).

■ ABBREVIATIONS

P3HT, poly(3-hexyl thiophene)
PS, polystyrene
OFET, organic field-effect transistor
M_n, number-average molecular weight
M_w, weight-average molecular weight

DOI: 10.1021/am507512m
ACS Appl. Mater. Interfaces 2015, 7, 1290−1297

SiO_2, silicon dioxide
AFM, atomic force microscopy
GIXD, grazing-incidence X-ray diffraction
OM, optical microscopy

REFERENCES

(1) Sirringhaus, H.; Kawase, T.; Friend, R. H.; Shimoda, T.; Inbasekaran, M.; Wu, W.; Woo, E. P. High-Resolution Inkjet Printing of All-Polymer Transistor Circuits. *Science* **2000**, *290*, 2123−2126.
(2) Yan, H.; Chen, Z.; Zheng, Y.; Newman, C.; Quinn, J. R.; Dötz, F.; Kastler, M.; Facchetti, A. A High-Mobility Electron-Transporting Polymer for Printed Transistors. *Nature* **2009**, *457*, 679−686.
(3) Yang, H.; LeFevre, S. W.; Ryu, C. Y.; Bao, Z. Solubility-Driven Thin Film Structures of Regioregular Poly(3-hexyl thiophene) Using Volatile Solvents. *Appl. Phys. Lett.* **2007**, *90*, 172116.
(4) Kline, R. J.; McGehee, M. D.; Toney, M. F. Highly Oriented Crystals at the Buried Interface in Polythiophene Thin-Film Transistors. *Nat. Mater.* **2006**, *5*, 222−228.
(5) Noh, Y.-Y.; Zhao, N.; Caironi, M.; Sirringhaus, H. Downscaling of Self-Aligned, All-Printed Polymer Thin-Film Transistors. *Nat. Nanotechnol.* **2007**, *2*, 784−789.
(6) Hamadani, B. H.; Gundlach, D. J.; McCulloch, I.; Heeney, M. Undoped Polythiophene Field-Effect Transistors with Mobility of 1 $cm^2V^{-1}s^{-1}$. *Appl. Phys. Lett.* **2007**, *91*, 243512.
(7) Wu, Y.; Liu, P.; Ong, B. S.; Srikumar, T.; Zhao, N.; Bottom, G.; Zhu, S. Controlled Orientation of Liquid-Crystalline Polythiophene Semiconductors for High-Performance Organic Thin-Film Transistors. *Appl. Phys. Lett.* **2005**, *86*, 142102.
(8) Jang, M.; Yang, H. Structural Control Over Self-Assembled Crystals of π-Conjugated Poly(3,3‴-didodecyl-quaterthiophene) for Organic Field-Effect Transistor Applications. *J. Nanosci. Nanotechnol.* **2012**, *12*, 1220−1225.
(9) Nielsen, C. B.; Turbiez, M.; McCulloch, I. Recent Advanced in the Development of Semiconducting DPP-Containing Polymers for Transistor Applications. *Adv. Mater.* **2013**, *25*, 1859−1880.
(10) Bronstein, H.; Chen, Z.; Ashraf, R. S.; Zhang, W.; Du, J.; Durrant, J. R.; Tuladhar, P. S.; Song, K.; Watkins, S. E.; Geerts, Y.; Wienk, M. M.; Janssen, R. A.; Anthopoulos, T.; Sirringhaus, H.; Heeney, M.; McCulloch, I. Thiono[3,2-*b*]thiophene-Diketopyrrolopyrrole-Containing Polymers for High-Performance Organic Field-Effect Transistors and Organic Photovoltaic Devices. *J. Am. Chem. Soc.* **2011**, *133*, 3272−3275.
(11) Huitema, H. E. A.; Gelinck, G. H.; van der Putten, J. B. P. H.; Kuijk, K. E.; Hart, C. M.; Cantatore, E.; Herwig, P. T.; van Breemen, A. J. J. M.; de Leeuw, D. M. Plastic Transistors in Active-Matrix Displays. *Nature* **2001**, *414*, 598−599.
(12) Huitema, H. E. A.; Gelinck, G. H.; van der Putten, J. B. P. H.; Kuijk, K. E.; Hart, K. M.; Cantatore, E.; de Leeuw, D. M. Active-Matrix Displays Driven by Solution Processed Polymeric Transistors. *Adv. Mater.* **2002**, *14*, 1201−1204.
(13) Dodabalapur, A. Organic and Polymer Transistors for Electronics. *Mater. Today* **2006**, *9*, 24−30.
(14) Janata, J.; Josowicz, M. Conducting Polymers in Electronics Chemical Sensors. *Nat. Mater.* **2003**, *2*, 19−24.
(15) Böhm, M.; Ullmann, A.; Zipperer, D.; Knobloch, A.; Glauert, W. H.; Fix, W. Printable Electronics for Polymer RFID Applications. *IEEE Int. Conf. Electron Devices Solid-State Circuits* **2006**, 1034−1041.
(16) Miozzo, L.; Yassar, A.; Horowitz, G. Surface Engineering for High Performance Organic Electronic Devices: The Chemical Approach. *J. Mater. Chem.* **2010**, *20*, 2513−2538.
(17) Dong, H.; Fu, X.; Liu, J.; Wang, Z.; Hu, W. 25th Anniversary Article: Key Points for High-Mobility Organic Field-Effect Transistors. *Adv. Mater.* **2013**, *25*, 6158−6183.
(18) Wang, Y.; Chen, Z.; Chen, J.; Qu, Y.; Yang, X. Miscibility, Crystallization, and Morphology of the Double-Crystalline Blends of Insulating Polyethylene and Semiconducting Poly(3-Butylthiophene). *J. Macromol. Sci., Part B: Phys.* **2013**, *52*, 1388−1404.
(19) Lu, G.; Tang, H.; Huan, Y.; Li, S.; Li, L.; Wang, Y.; Yang, X. Enhanced Charge Transportation in Semiconducting Polymer/Insulating Polymer Composites: The Role of an Interpenetrating Bulk Interface. *Adv. Funct. Mater.* **2010**, *20*, 1714−1720.
(20) Lim, J. A.; Kim, J.-H.; Qiu, L.; Lee, W. H.; Lee, H. S.; Kwak, D.; Cho, K. Inkjet-Printed Single-Droplet Organic Transistors Based on Semiconductor Nanowires Embedded in Insulating Polymers. *Adv. Funct. Mater.* **2010**, *20*, 3292−3297.
(21) Lu, G.; Blakesley, J.; Himmelberger, S.; Pingel, P.; Frisch, J.; Lieberwirth, I.; Salzmann, I.; Oehzelt, M.; Pietro, R. D.; Salleo, A.; Koch, N.; Neher, D. Moderate Doping Leads to High Performance of Semiconductor/Insulator Polymer Blend Transistors. *Nat. Commun.* **2013**, *4*, 1588.
(22) Wang, X.; Lee, W. H.; Zhang, G.; Wang, X.; Kang, B.; Lu, H.; Qiu, L.; Cho, K. Self-Stratified Semiconductor/Dielectric Polymer Blends: Vertical Phase Separation for Facile Fabrication of Organic Transistors. *J. Mater. Chem. C* **2013**, *1*, 3989−3998.
(23) Arias, A. C.; Endicott, F.; Street, R. A. Surface-Induced Self-Encapsulation of Polymer Thin-Film Transistors. *Adv. Mater.* **2006**, *18*, 2900−2904.
(24) Sun, T.; Jung, B.-J.; Lee, T.; Berger, L.; Huang, J.; Liu, L.; Reich, D. H.; Katz, H. E. Tunability of Mobility and Conductivity over Large Ranges in Poly(3,3‴-didodecylquaterthiophene)/Insulating Polymer Composites. *ACS Appl. Mater. Interfaces* **2009**, *1*, 412−419.
(25) Li, G.; Zhu, R.; Yang, Y. Polymer Solar Cells. *Nat. Photonics* **2012**, *6*, 153−161.
(26) Goffri, S.; Muller, C.; Stingelin-Stutzmann, N.; Breiby, D. W.; Radano, C. P.; Andreasen, J. W.; Thompson, R.; Janssen, R. A. J.; Nielsen, M. M.; Smith, P.; Sirringhaus, H. Multicomponent Semiconducting Polymer Systems with Low Crystallization-Induced Percolation Threshold. *Nat. Mater.* **2006**, *5*, 950−956.
(27) Nilsson, S.; Bernasik, A.; Budkowski, A.; Moons, E. Morphology and Phase Segregation of Spin-Casted Films of Polyfluorene/PCBM Blends. *Macromolecules* **2007**, *40*, 8291−8301.
(28) Jeffries-El, M.; Sauvé, G.; McCullough, R. D. In-Situ End-Group Functionalization of Regioregular Poly(3-alkylthiophene) Using the Grignard Metathesis Polymerization Method. *Adv. Mater.* **2004**, *16*, 1017−1019.
(29) Kim, S. H.; Jang, M.; Yang, H.; Anthony, J. E.; Park, C. E. Physicochemically Stable Polymer-Coupled Oxide Dielectrics for Multipurpose Organic Electronic Applications. *Adv. Funct. Mater.* **2011**, *21*, 2198−2207.
(30) Aiyar, A. R.; Hong, J. I.; Nambiar, R.; Collard, D. M.; Reichmanis, E. Tunable Crystallinity in Regioregular Poly(3-Hexylthiophene) Thin Films and Its Impact on Field Effect Mobility. *Adv. Funct. Mater.* **2011**, *21*, 2652−2659.
(31) Aiyar, A. R.; Hong, J. I.; Izumi, J.; Choi, D.; Kleinhenz, N.; Reichmanis, E. Ultrasound-Induced Ordering in Poly(3-hexylthiophene): Role of Molecular and Process Parameters on Morphology and Charge Transport. *ACS Appl. Mater. Interfaces* **2013**, *5*, 2368−2377.
(32) Kim, B.-G.; Kim, M.-S.; Kim, J. Ultrasonic-Assisted Nanodimensional Self-Assembly of Poly-3-hexylthiophene for Organic Photovoltaic Cells. *ACS Nano* **2010**, *4*, 2160−2166.
(33) Hintz, H.; Egelhaaf, H. J.; Peisert, H.; Chassé, T. Photo-Oxidation and Ozonization of Poly(3-hexylthiophene) Thin Films as Studied by UV/VIS and Photoelectron Spectroscopy. *Polym. Degrad. Stab.* **2010**, *95*, 818−825.
(34) He, M.; Ge, J.; Fang, M.; Qiu, F.; Yang, Y. Fabricating Polythiophene into Highly Aligned Microwire Film by Fast Evaporation of Its Whisker Solution. *Polymer* **2010**, *51*, 2236−2243.
(35) Yamamoto, T.; Komarudin, D.; Arai, M.; Lee, B.-L.; Suganuma, H.; Asakawa, N.; Inoue, Y.; Kubota, K.; Sasaki, S.; Fukuda, T.; Matsuda, H. Extensive Studies on π-Stacking of Poly(3-alkylthiophene-2,5-diyl)s and Poly(4-alkylthiazole-2,5-diyl)s by Optical Spectroscopy, NMR Analysis, Light Scattering Analysis, and X-ray Crystallography. *J. Am. Chem. Soc.* **1998**, *120*, 2047−2058.

DOI: 10.1021/am507512m
ACS Appl. Mater. Interfaces 2015, 7, 1290−1297

(36) Lee, J. N.; Park, C.; Whitesides, G. M. Solvent Compatibility of Poly(dimethylsiloxane)-Based Microfluidic Devices. *Anal. Chem.* **2003**, *75*, 6544−6554.
(37) Longjian, X.; Xiang, G.; Kui, Z.; Jiangang, L.; Xinhong, Y.; Yanchun, H. The Formation of Different Structures of Poly(3-hexylthiophene) Film on a Patterned Substrate by Dip Coating from Aged Solution. *Nanotechnology* **2010**, *21*, 145303.
(38) Qiu, L.; Lee, W. H.; Wang, X.; Kim, J. S.; Lim, J. A.; Kwak, D.; Lee, S.; Cho, K. Organic Thin-film Transistors Based on Polythiophene Nanowires Embedded in Insulating Polymer. *Adv. Mater.* **2009**, *21*, 1349−1353.
(39) Lim, J. A.; Kim, J.-H.; Qiu, L.; Lee, W. H.; Lee, H. S.; Kwak, D.; Cho, K. Inkjet-Printed Single-Droplet Organic Transistors Based on Semiconductor Nanowires Embedded in Insulating Polymers. *Adv. Funct. Mater.* **2010**, *20*, 3292−3297.
(40) Park, Y. D.; Kim, D. H.; Jang, Y.; Cho, J. H.; Hwang, M.; Lee, H. S.; Lim, J. A.; Cho, K. Effect of Side Chain Length on Molecular Ordering and Field-Effect Mobility in Poly(3-alkylthiophene) Transistors. *Org. Electron.* **2006**, *7*, 514−520.
(41) Yang, H.; Shin, T. J.; Bao, Z.; Ryu, C. Y. Structural Transitions of Nanocrystalline Domains in Regioregular Poly(3-hexyl thiophene) Thin Films. *J. Polym. Sci., Part B: Polym. Phys.* **2007**, *45*, 1303−1312.

DOI: 10.1021/am507512m
ACS Appl. Mater. Interfaces 2015, 7, 1290−1297